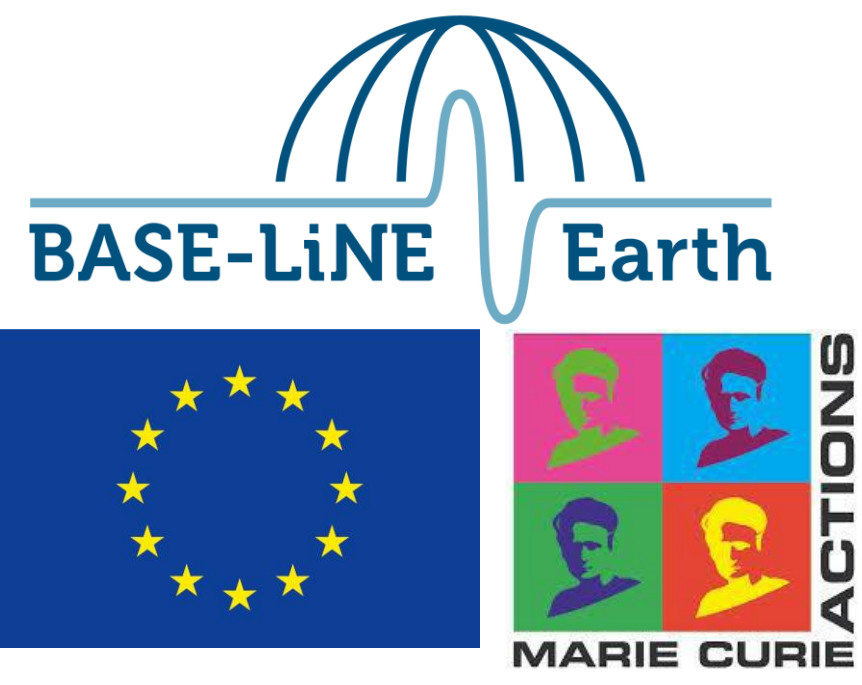


Oxygen isotope exchange kinetics during high-temperature synthesis of dolomite and magnesite



Isaac Kell-Duivestain ¹, Andre Baldermann ¹, Martin Dietzel ¹, Vasileios Mavromatis ¹, Albrecht Leis ²

¹ Institute of Applied Geosciences, Graz University of Technology, Graz, Austria; ² JR Aqua Consol, Graz, Austria

Contact lead author by email: isaac.kellduivestain@tugraz.at or phone: +43 (316) 873 - 6857



1 – Summary

Oxygen isotopes are a useful tool for interpreting paleotemperatures of marine environments where sedimentary Ca-Mg-carbonates such as magnesite and dolomite are formed. Until now no studies have experimentally investigated the kinetic behaviour of oxygen isotope exchange between dolomite - water and magnesite - water. Therefore in this study, hydrothermal precipitation experiments were performed in order to trace the evolution of $\delta^{18}\text{O}$ signatures as well as the mineralogical phases during the transformation of CaCO_3 seeds to dolomite and magnesite through intermediate, metastable Ca-Mg carbonate phases. Herein we present data from over a hundred recent dolomitization experiments conducted at temperatures of 150, 180 and 220 °C over the course of one year.

2 – Experimental setup and reactor conditions

Dolomite and magnesite were synthesized in Teflon lined autoclaves at temperatures of 150, 180 and 220 °C by reacting finely ground (10 – 40 μm) either inorganic calcite or speleothem aragonite and NaHCO_3 with a synthetic MgCl_2 solution (concentrations given in **Table 1**) over the course of one year.

The MgCl_2 solution was highly depleted in oxygen-18 ($\delta^{18}\text{O}_{\text{VSMOW}} = -46.4\text{‰}$) so that the evolution of solid $\delta^{18}\text{O}$ values could be traced with high precision and isotope equilibrium could be clearly established: hence allowing for kinetics of the oxygen isotope exchange during hydrothermal formation of magnesite and dolomite to be determined experimentally for the first time.

pH and Ca-Mg-carbonate SI values were modelled with respect to reactive temperature and measured aqueous Ca, Mg, Na, Cl and HCO_3^- concentrations using PHREEQC and it's associated LLNL database. **Table 2** (below) summarises the basic aqueous chemistry of the experiments once at a stable state with respect to their mineralogy and oxygen isotope composition.

Figure 1: experimental setup

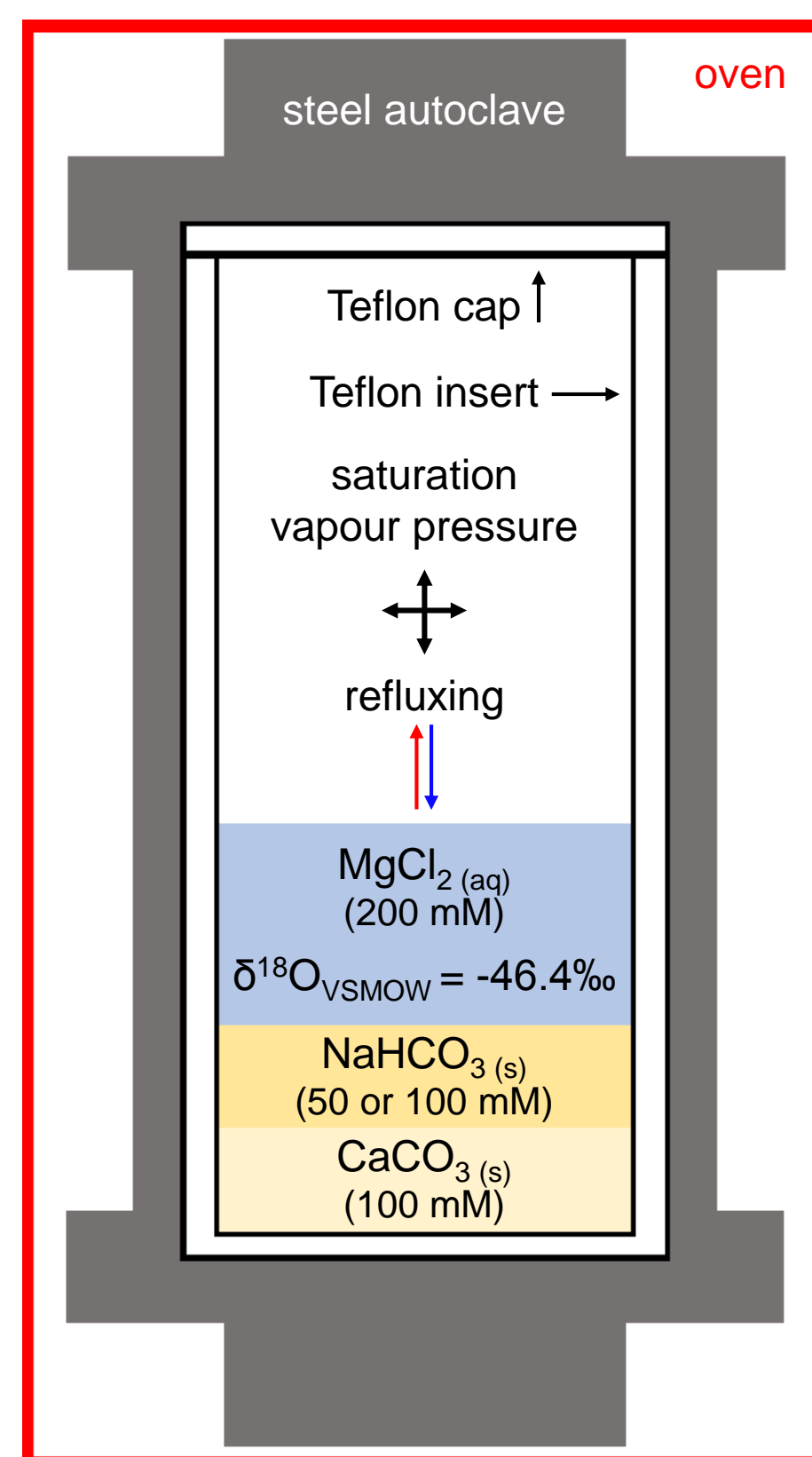


Figure 1. Schematic of experimental setup.

Table 1: Summary of initial reactant concentrations. The blue, red and black squares and circles serve as the legend for all further figures on this poster representing samples from the respective experimental: i.e. Ct-100 (full squares), Agt-100 (full circles) & Agt-50 (empty circles) and temperature 150°C (blue), 180°C (red) and 220°C (black). The calcite reactant was synthetically produced in house, the aragonite is from highly pure aragonitic speleothems. $\delta^{18}\text{O}$ of the fluid is reported relative to the VPDB standard for easy comparison with that of the CaCO_3 reactant phase.

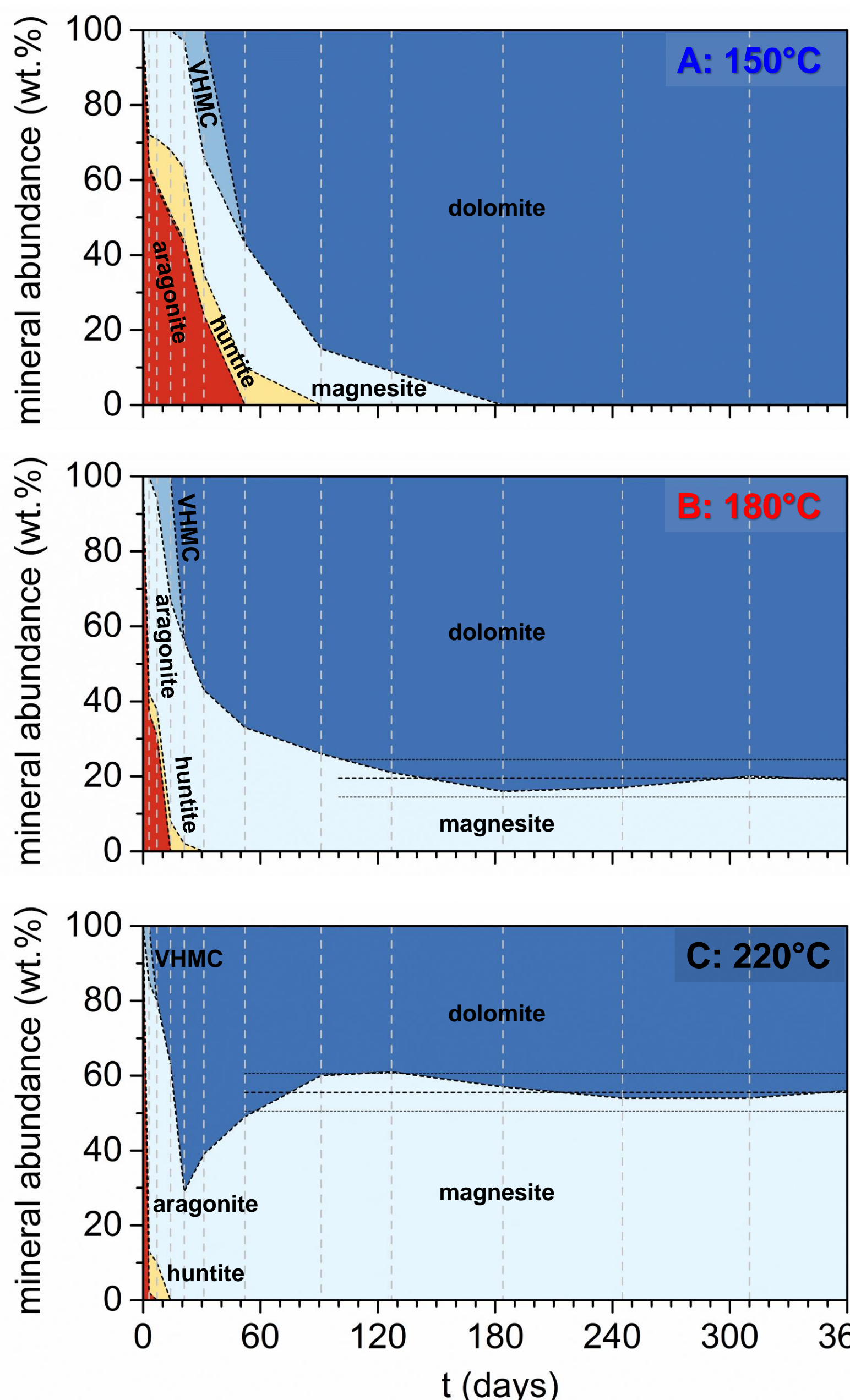
| Set ID * | Reactant CaCO_3 phase | CaCO_3 | | NaHCO_3 | | MgCl_2 | | $\delta^{18}\text{O}_{\text{VPDB}} (\text{‰})$ | | N at: | | |
|----------|--------------------------------|-----------------|-----|------------------|-----|-----------------|-----|--|-----------------|-------|-------|-------|
| | | mg | mM | mg | mM | mL | mM | CaCO_3 | MgCl_2 | 150°C | 180°C | 220°C |
| Ct-100 | calcite | 330 | 100 | 250 | 100 | 30.3 | 200 | -17.49 | -75.01 | - | 20 | 20 |
| Agt-100 | aragonite | 330 | 100 | 250 | 100 | 30.3 | 200 | -6.38 | -75.01 | - | 20 | 20 |
| Agt-50 | aragonite | 330 | 100 | 125 | 50 | 30.3 | 200 | -6.38 | -75.01 | 20 | 20 | 20 |

Table 2: Summary of aqueous chemistry conditions when reactors are heated and mineralogy has reached an apparent stable state. Saturation indices were modelled with PHREEQC and its associated LLNL database. Errors are given as $\pm 1\sigma$.

| T (°C) | pH | [Ca] (mM) | [Mg] (mM) | [HCO_3^-] (mM) | Ca/Mg (molar) | SI dolomite | SI magnesite | SI calcite | SI aragonite |
|--------|---------------|------------|-------------|---------------------------|-----------------|---------------|---------------|---------------|---------------|
| 150 | 6.5 \pm 0.2 | 41 \pm 3 | 141 \pm 5 | 0.1 \pm 0.1 | 0.29 \pm 0.02 | 4.1 \pm 0.3 | 2.0 \pm 0.2 | 0.9 \pm 0.2 | 0.8 \pm 0.2 |
| 180 | 6.3 \pm 0.1 | 50 \pm 4 | 98 \pm 6 | 0.1 \pm 0.1 | 0.51 \pm 0.04 | 4.4 \pm 0.4 | 2.1 \pm 0.2 | 1.2 \pm 0.2 | 1.1 \pm 0.2 |
| 220 | 6.0 \pm 0.2 | 71 \pm 5 | 88 \pm 5 | 0.1 \pm 0.1 | 0.81 \pm 0.07 | 4.2 \pm 0.5 | 2.0 \pm 0.2 | 1.3 \pm 0.2 | 1.2 \pm 0.2 |

3 – Mineralogy

Figure 2: precipitate mineralogy vs. time



All experimental sets precipitated dolomite along with varied amounts of magnesite via a stepwise dissolution-recrystallisation reaction sequence adhering to Ostwald's step rule. Representative examples from experimental set Agt-50 at each reaction temperature are shown in **Figure 2** (left).

Higher temperatures experiments yielded increased magnesite vs. dolomite compared to lower temperature experiments as can be seen in **Figure 3** (below).

Figure 3: magnesite : dolomite vs. time

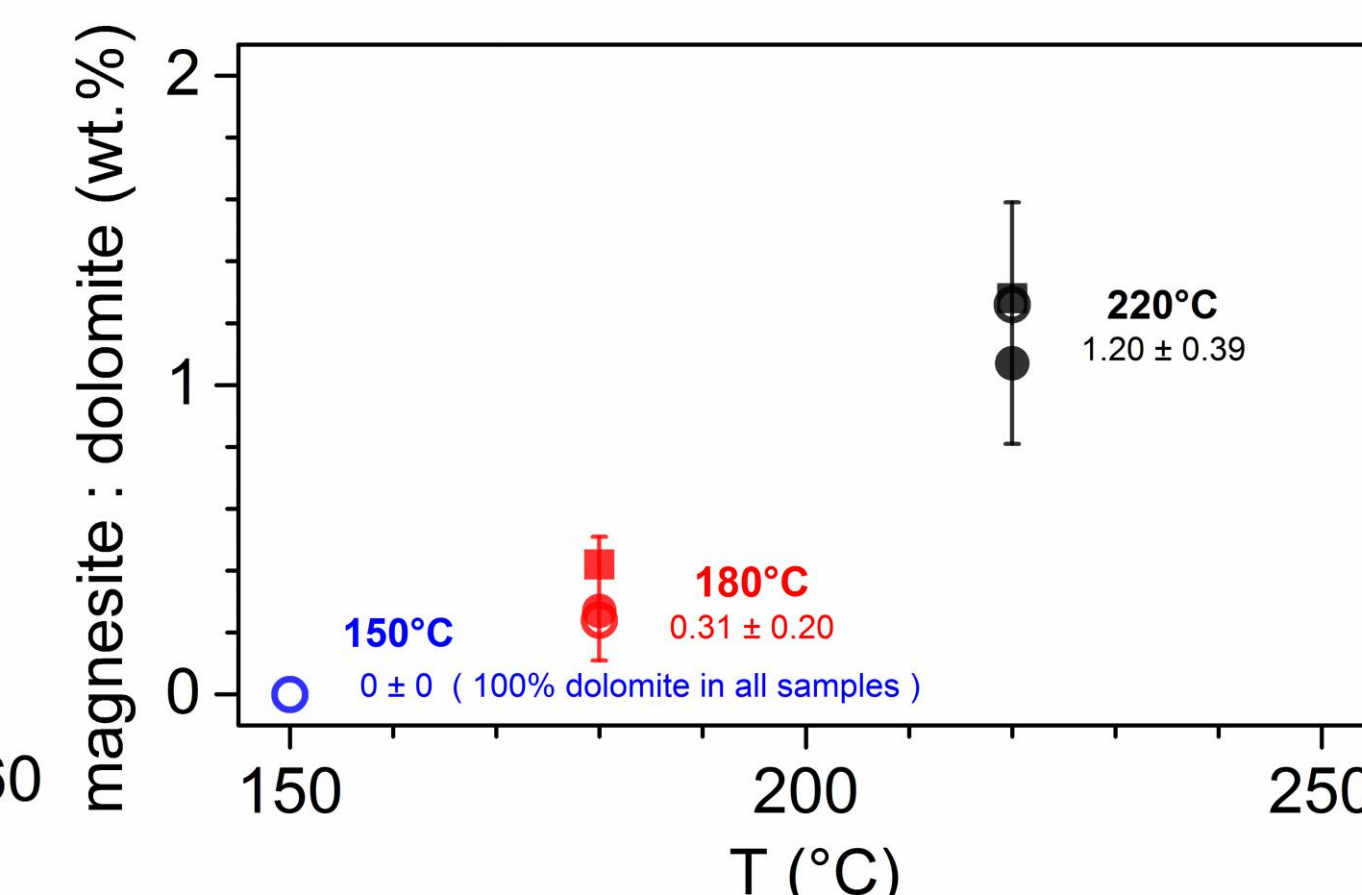


Figure 3: magnesite : dolomite ratios of bulk precipitates (wt.%) when experiments are at an apparently stable state w.r.t. mineralogy, error bars are given as 2 σ .

4 – Oxygen isotope exchange kinetics

Figure 4: $\delta^{18}\text{O}$ vs. reaction time

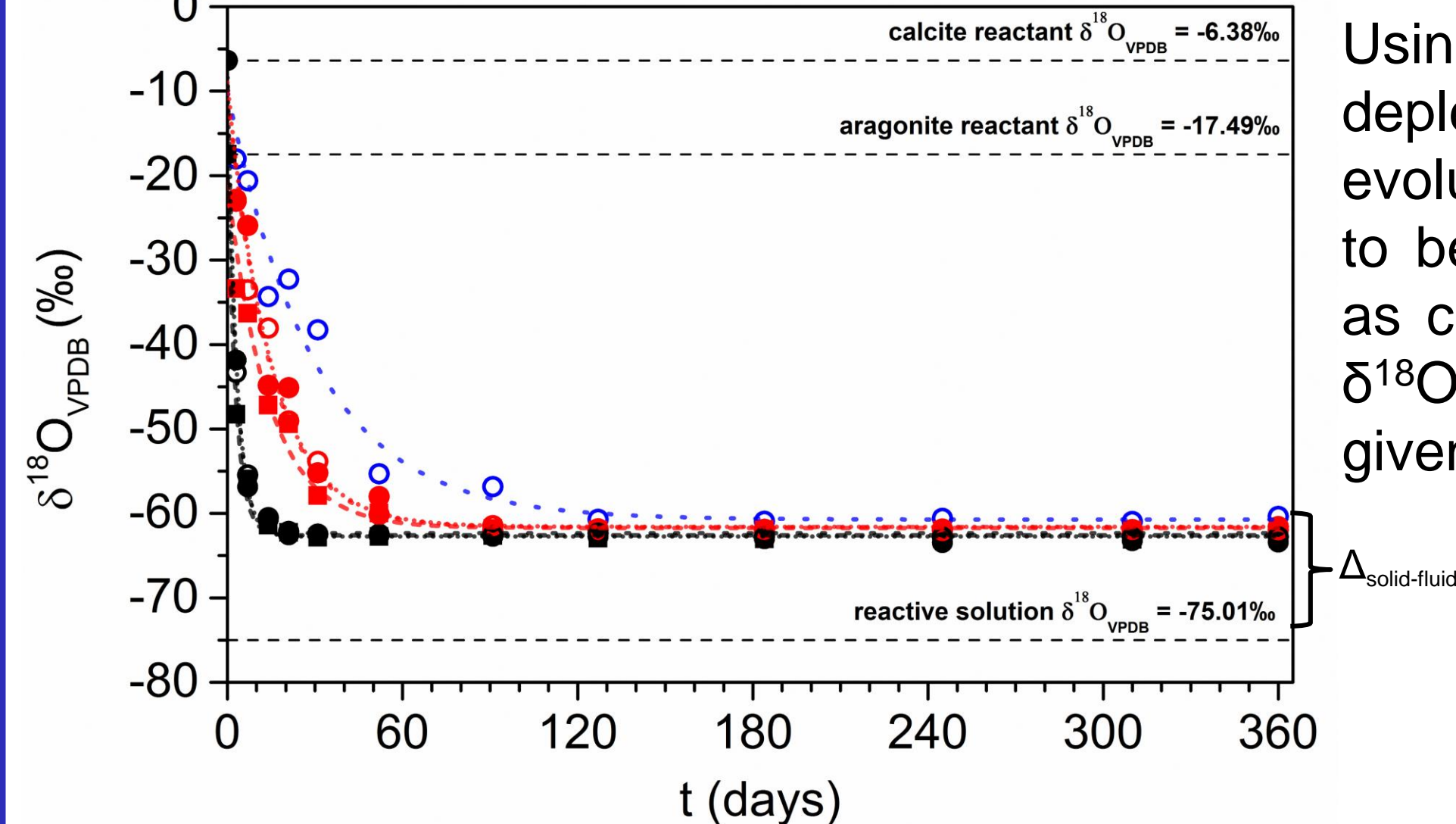


Figure 4. Evolution of $\delta^{18}\text{O}_{\text{VPDB}}$ with reaction time. The dashed black lines indicate the $\delta^{18}\text{O}_{\text{VPDB}}$ values of the initial reactants. $\delta^{18}\text{O}_{\text{VPDB}}$ and $\Delta_{\text{precipitate-solution}}$ values at equilibrium are provided in table X. Error is contained within the marker size.

Using a reactive solution highly depleted in ^{18}O allowed for the evolution of precipitate $\delta^{18}\text{O}$ values to be followed with high precision as can be seen in **Figure 4** (left). $\delta^{18}\text{O}$ and $\Delta_{\text{precipitate-solution}}$ values are given in **Table 3** (below).

Table 3: $\delta^{18}\text{O}_{\text{VPDB}}$ and $\Delta_{\text{precipitate-solution}}$ values at isotope equilibrium ($\pm 1\sigma$). Values are average for all experimental sets at given temperature.

| T (°C) | $\delta^{18}\text{O}_{\text{VPDB}} (\text{‰})$ (at - equilibrium) | $\Delta_{\text{solid-fluid}} (\text{‰})$ (at - equilibrium) |
|--------|---|---|
| 150 | -60.7 \pm 0.2 | 14.3 \pm 0.2 |
| 180 | -62.0 \pm 0.1 | 13.1 \pm 0.1 |
| 220 | -63.0 \pm 0.2 | 12.0 \pm 0.2 |

Figure 5: $\delta^{18}\text{O}$ exchange as pseudo-first-order reaction

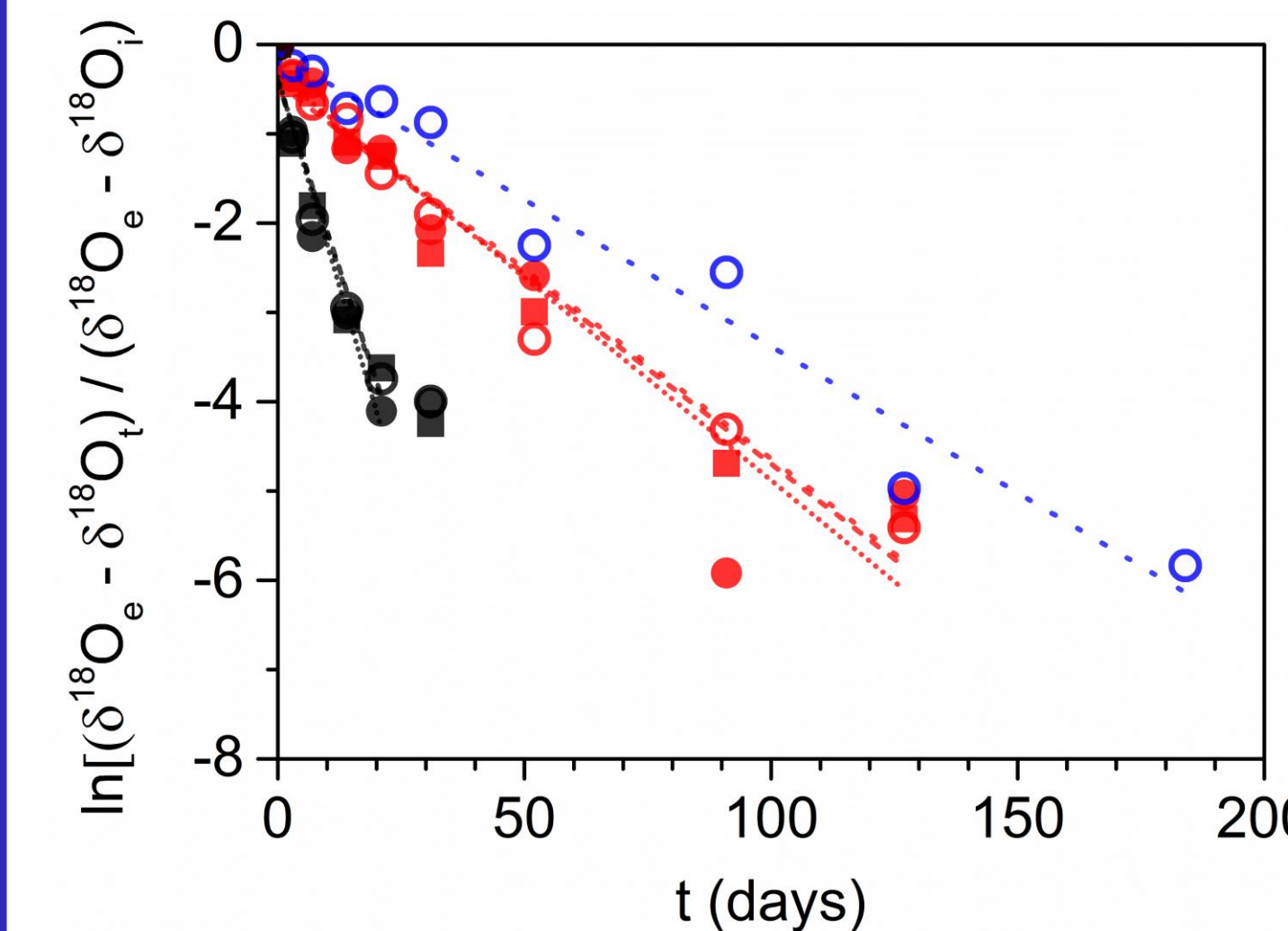


Figure 5: $\delta^{18}\text{O}$ as pseudo-first-order reaction. Regression lines have the form $\ln(x) = -kt$, where k is the pseudo-first-order kinetic coefficient and the slope of the regression lines is equal to -k.

Figure 6: Arrhenius plot of ^{18}O exchange rates

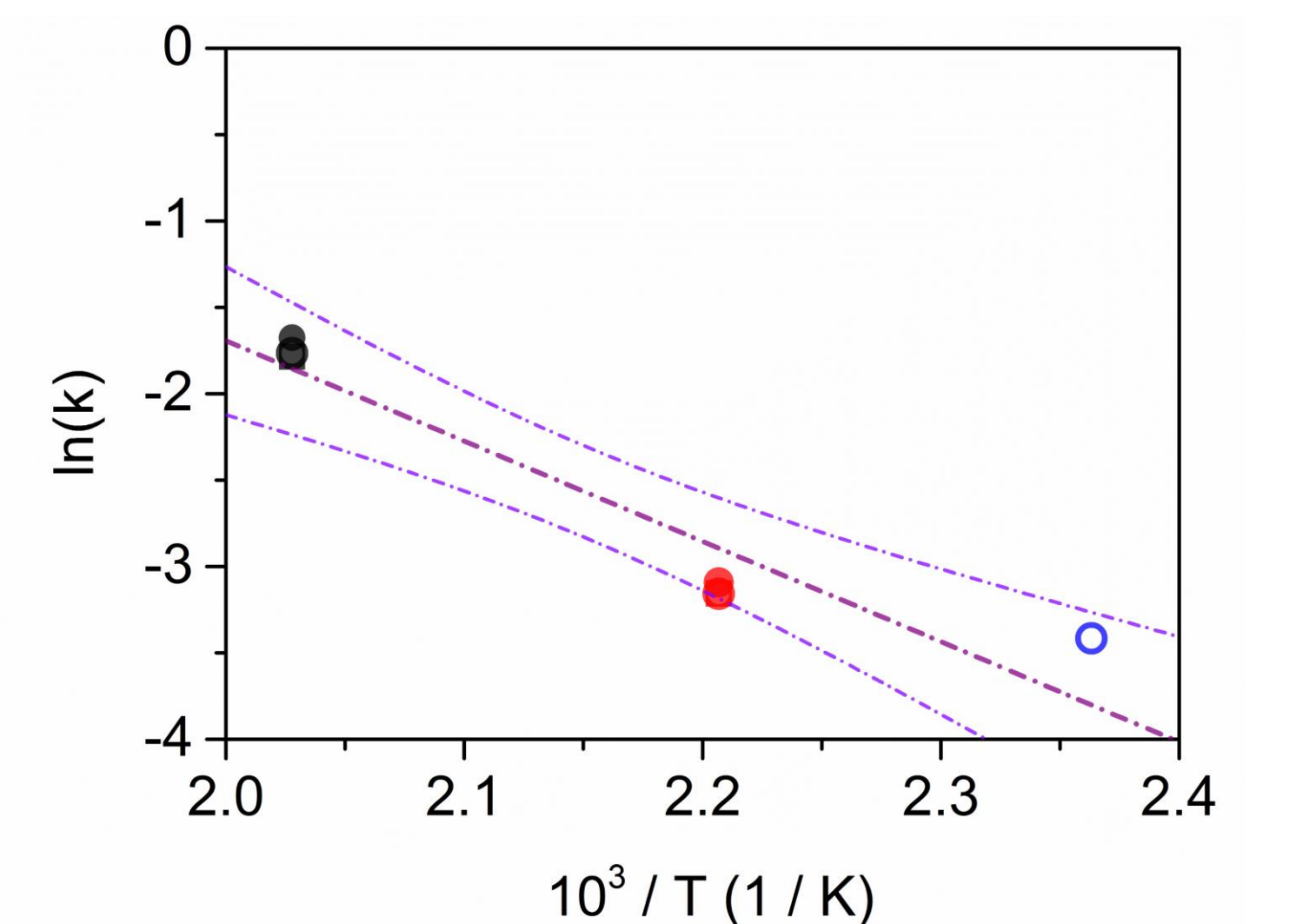


Figure 6: Arrhenius cross plot of the pseudo-first-order kinetic coefficients

Analysis of the oxygen isotope exchange as a pseudo-first-order reaction (**Figure 5**) allowed for pseudo-first-order kinetic coefficients 'k' (days⁻¹), $t_{0.5}$ and $t_{0.999}$ times (days) to be calculated based on experimental results for the first time (**Table 4**). The rate of oxygen isotope exchange increased with temperature following the Arrhenius relationship (**Figure 6**) which in turn allowed for the apparent activation energy (E_a) for oxygen isotope fractionation during dolomitization to also be determined for the first time. $E_a = 48.4 \pm 7.2 \text{ kJ}\cdot\text{mol}^{-1}$.

Table 4: Summary of oxygen isotope exchange kinetics and apparent activation energy. k is the reaction coefficient, $t_{0.5}$ and $t_{0.999}$ are the times required to reach 50 and 99.9 % of isotope equilibrium.

| T (°C) | k (days ⁻¹) | $t_{0.5}$ (days) | $t_{0.999}$ (days) |
|--------|-------------------------|------------------|--------------------|
| 150 | 0.033 \pm 0.002 | 21 \pm 3 | 211 \pm 20 |
| 180 | 0.044 \pm 0.002 | 16 \pm 2 | 160 \pm 12 |
| 220 | 0.175 \pm 0.010 | 4 \pm 1 | 40 \pm 5 |

5 – Oxygen isotope fractionation

Figure 7: $10^3 \ln(\alpha_{\text{precipitate-solution}})$ vs. $10^6/T^2$

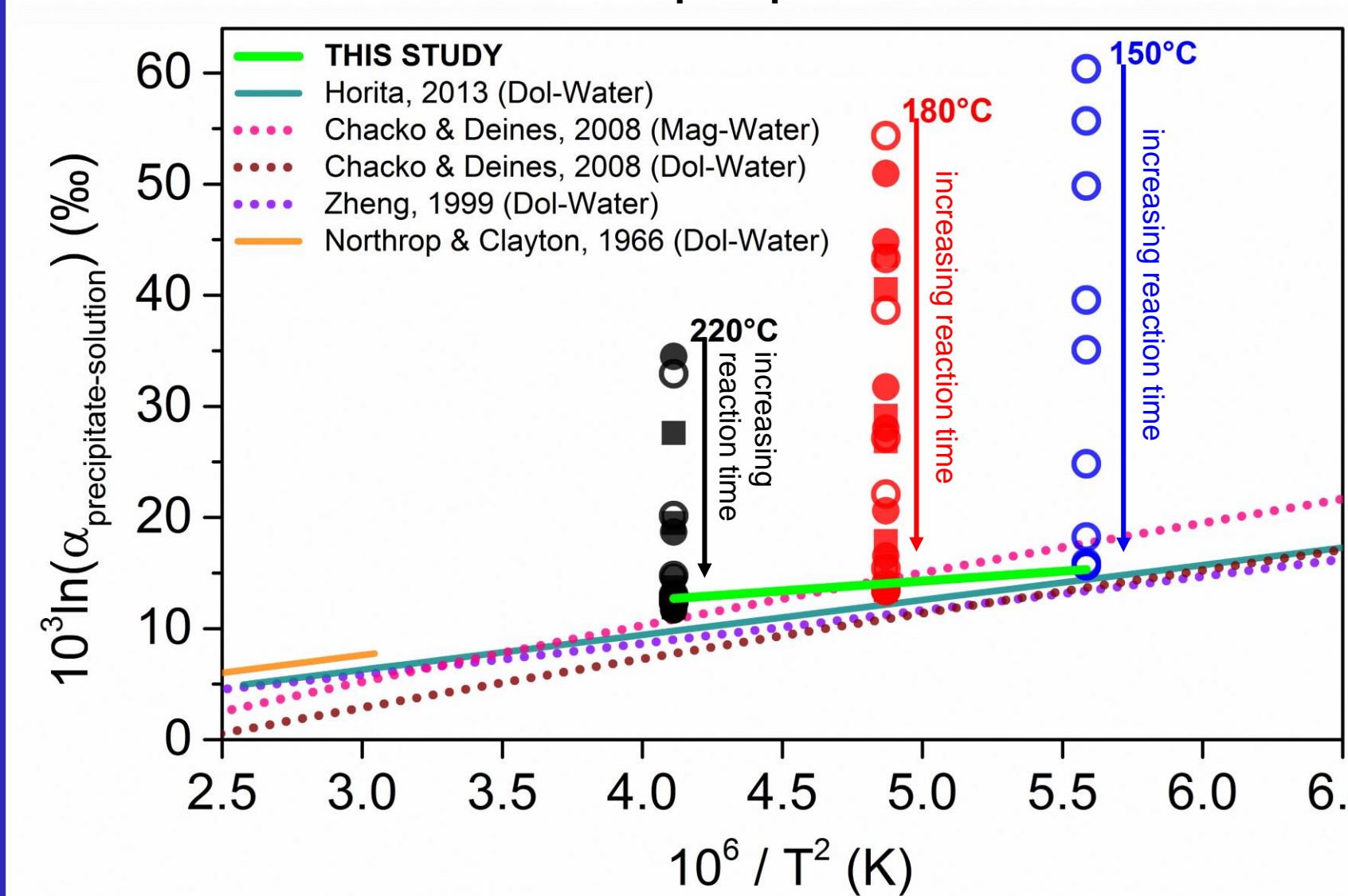


Figure 7: Fractionation line for $\delta^{18}\text{O}$ between precipitated Ca-Mg-carbonates (magnesite + dolomite) and water from this study (green line) compared to existing experimental (solid lines) and theoretical (dashed lines) fractionation lines for dolomite-water and magnesite-water from the literature. Markers running vertically down (black, red and blue) show the evolution of $10^3 \ln(\alpha)$ towards equilibrium with time.

We obtained from our data an overall isotope fractionation factor $10^3 \ln(\alpha) = 2.702(\pm 0.236) \cdot (10^6/T^2) + 0.436(\pm 1.290)$ which is generally consistent with the literature, sitting between fractionation lines for dolomite - water and magnesite - water (**Figure 7**).

6 – Conclusions and outlook

1. The novel application of a reactive solution highly depleted in ^{18}O allowed for the oxygen isotope fractionation to be followed precisely and equilibrium established.
2. Analysis of oxygen isotope exchange as a pseudo-first-order reaction allowed for reaction rate coefficients (k) and the time to reach 99.9% of isotope equilibrium ($t_{0.999}$) during dolomitization to be determined for the first time. Reaction rates increased following the Arrhenius relationship which allowed the apparent activation energy for oxygen isotope exchange to be determined ($48.4 \pm 7.2 \text{ kJ}\cdot\text{mol}^{-1}$).
3. Despite the use of different experimental conditions, and subsequently different mineralogy precipitated, the kinetics of oxygen isotope exchange was the same at equal temperatures, isolating temperature as the sole control over kinetics in our experimental approach.

Further work to separate the co-precipitated dolomite and magnesite using di-Na-EDTA is ongoing to that the oxygen isotope fractionation can be investigated in the individual phases as opposed to the mixture.